Research Article | Vol. 26, No. 3 | 5 Feb 2018 | OPTICS EXPRESS 2509
Optics EXPRESS

Generation of high-field terahertz pulses in an HMQ-TMS organic crystal pumped by an ytterbium laser at 1030 nm

ANDREA ROVERE,[1] YOUNG-GYUN JEONG,[1] RICCARDO PICCOLI,[1] SEUNG-HEON LEE,[2] SEUNG-CHUL LEE,[2] O-PIL KWON,[2] MOJCA JAZBINSEK,[3] ROBERTO MORANDOTTI,[1,4,5] AND LUCA RAZZARI[1,*]

[1]*INRS - Énergie, Matériaux et Télécommunications, 1650 Blvd Lionel Boulet, Varennes, J3X 1S2 (Québec), Canada*
[2]*Department of Molecular Science and Technology, Ajou University, Suwon 16499, South Korea*
[3]*Institute of Computational Physics, Zurich University of Applied Sciences (ZHAW), 8401 Winterthur, Switzerland*
[4]*National Research University of Information Technologies, Mechanics and Optics, 199034 St. Petersburg, Russia*
[5]*Institute of Fundamental and Frontier Sciences, University of Electronic Science and Technology of China, Chengdu 610054, China*
[*]*razzari@emt.inrs.ca*

Abstract: We present the generation of high-peak-electric-field terahertz pulses via collinear optical rectification in a 2-(4-hydroxy-3-methoxystyryl)-1-methilquinolinium-2,4,6-trimethylbenzenesulfonate (HMQ-TMS) organic crystal. The crystal is pumped by an amplified ytterbium laser system, emitting 170-fs-long pulses centered at 1030 nm. A terahertz peak electric field greater than 200 kV/cm is obtained for 420 μJ of optical pump energy, with an energy conversion efficiency of 0.26% - about two orders of magnitude higher than in common inorganic crystals collinearly pumped by amplified femtosecond lasers. An open-aperture Z-scan measurement performed on an n-doped InGaAs thin film using such terahertz source shows a nonlinear increase in the terahertz transmission of about 2.2 times. Our findings demonstrate the potential of this terahertz generation scheme, based on ytterbium laser technology, as a simple and efficient alternative to the existing intense table-top terahertz sources. In particular, we show that it can be readily used to explore nonlinear effects at terahertz frequencies.

OCIS codes: (140.3615) Lasers, ytterbium; (190.0190) Nonlinear optics; (040.2235) Far infrared or terahertz; (190.4710) Optical nonlinearities in organic materials; (300.6500) Spectroscopy, time-resolved.

References and links

1. H. A. Hafez, X. Chai, A. Ibrahim, S. Mondal, D. Férachou, X. Ropagnol, and T. Ozaki, "Intense terahertz radiation and their applications," J. Opt. **18**(9), 093004 (2016).
2. S. L. Dexheimer, *Terahertz spectroscopy: principles and applications* (CRC, 2007).
3. S. J. Oh, J. Choi, I. Maeng, J. Y. Park, K. Lee, Y.-M. Huh, J.-S. Suh, S. Haam, and J.-H. Son, "Molecular imaging with terahertz waves," Opt. Express **19**(5), 4009–4016 (2011).
4. I. F. Akyildiz, J. M. Jornet, and C. Han, "Terahertz band: next frontier for wireless communications," Phys. Commun. **12**, 16–32 (2014).
5. P. F. Taday, "Applications of terahertz spectroscopy to pharmaceutical sciences," Philos. Trans. A Math. Phys. Eng. Sci. **362**(1815), 351–364 (2004).
6. J. F. Federici, B. Schulkin, F. Huang, D. Gary, R. Barat, F. Oliveira, and D. Zimdars, "THz imaging and sensing for security applications - explosives, weapons and drugs," Semicond. Sci. Technol. **20**(7), S266–S280 (2005).
7. T. Yasui, T. Yasuda, K. Sawanaka, and T. Araki, "Terahertz paintmeter for noncontact monitoring of thickness and drying progress in paint film," Appl. Opt. **44**(32), 6849–6856 (2005).
8. Q. Wu, T. D. Hewitt, and X.-C. Zhang, "Two-dimensional electro-optic imaging of THz beams," Appl. Phys. Lett. **69**(8), 1026–1028 (1996).
9. Z. Jiang and X.-C. Zhang, "Single-shot spatiotemporal terahertz field imaging," Opt. Lett. **23**(14), 1114–1116 (1998).

#314567 https://doi.org/10.1364/OE.26.002509
Journal © 2018 Received 29 Nov 2017; revised 12 Jan 2018; accepted 13 Jan 2018; published 23 Jan 2018

Optics EXPRESS

10. F. Blanchard, A. Doi, T. Tanaka, H. Hirori, H. Tanaka, Y. Kadoya, and K. Tanaka, "Real-time terahertz near-field microscope," Opt. Express **19**(9), 8277–8284 (2011).
11. T. L. Cocker, D. Peller, P. Yu, J. Repp, and R. Huber, "Tracking the ultrafast motion of a single molecule by femtosecond orbital imaging," Nature **539**(7628), 263–267 (2016).
12. R. Ulbricht, E. Hendry, J. Shan, T. F. Heinz, and M. Bonn, "Carrier dynamics in semiconductors studied with time-resolved terahertz spectroscopy," Rev. Mod. Phys. **83**(2), 543–586 (2011).
13. H. A. Hafez, I. Al-Naib, M. M. Dignam, Y. Sekine, K. Oguri, F. Blanchard, D. G. Cooke, S. Tanaka, F. Komori, H. Hibino, and T. Ozaki, "Nonlinear terahertz field-induced carrier dynamics in photoexcited epitaxial monolayer graphene," Phys. Rev. B **91**(3), 035422 (2015).
14. F. Giorgianni, E. Chiadroni, A. Rovere, M. Cestelli-Guidi, A. Perucchi, M. Bellaveglia, M. Castellano, D. Di Giovenale, G. Di Pirro, M. Ferrario, R. Pompili, C. Vaccarezza, F. Villa, A. Cianchi, A. Mostacci, M. Petrarca, M. Brahlek, N. Koirala, S. Oh, and S. Lupi, "Strong nonlinear terahertz response induced by Dirac surface states in Bi_2Se_3 topological insulator," Nat. Commun. **7**, 11421 (2016).
15. R. Matsunaga and R. Shimano, "Nonequilibrium BCS state dynamics induced by intense terahertz pulses in a superconducting NbN film," Phys. Rev. Lett. **109**(18), 187002 (2012).
16. T. Kubacka, J. A. Johnson, M. C. Hoffmann, C. Vicario, S. de Jong, P. Beaud, S. Grübel, S.-W. Huang, L. Huber, L. Patthey, Y.-D. Chuang, J. J. Turner, G. L. Dakovski, W.-S. Lee, M. P. Minitti, W. Schlotter, R. G. Moore, C. P. Hauri, S. M. Koohpayeh, V. Scagnoli, G. Ingold, S. L. Johnson, and U. Staub, "Large-amplitude spin dynamics driven by a THz pulse in resonance with an electromagnon," Science **343**(6177), 1333–1336 (2014).
17. A. Nahata, A. S. Weling, and T. F. Heinz, "A wideband coherent terahertz spectroscopy system using optical rectification and electro-optic sampling," Appl. Phys. Lett. **69**(16), 2321–2323 (1996).
18. F. Blanchard, G. Sharma, L. Razzari, X. Ropagnol, H. C. Bandulet, F. Vidal, R. Morandotti, J. C. Kieffer, T. Ozaki, H. Tiedje, H. Haugen, M. Reid, and F. Hegmann, "Generation of intense terahertz radiation via optical methods," IEEE J. Quantum Electron. **17**(1), 5–16 (2011).
19. Y. J. Ding, "High-Power Tunable Terahertz Sources Based on Parametric Processes and Applications," IEEE J. Sel. Top. Quantum Electron. **13**(3), 705–720 (2007).
20. D. Creeden, J. C. McCarthy, P. A. Ketteridge, P. G. Schunemann, T. Southward, J. J. Komiak, and E. P. Chicklis, "Compact, high average power, fiber-pumped terahertz source for active real-time imaging of concealed objects," Opt. Express **15**(10), 6478–6483 (2007).
21. H. Hirori, A. Doi, F. Blanchard, and K. Tanaka, "Single-cycle terahertz pulses with amplitudes exceeding 1 MV/cm generated by optical rectification in $LiNbO_3$," Appl. Phys. Lett. **98**(9), 091106 (2011).
22. J. Hebling, G. Almási, I. Kozma, and J. Kuhl, "Velocity matching by pulse front tilting for large area THz-pulse generation," Opt. Express **10**(21), 1161–1166 (2002).
23. J. A. Fülöp, G. Polónyi, B. Monoszlai, G. Andriukaitis, T. Balciunas, A. Pugzlys, G. Arthur, A. Baltuska, and J. Hebling, "Highly efficient scalable monolithic semiconductor terahertz pulse source," Optica **3**(10), 1075–1078 (2016).
24. A. Schneider, M. Neis, M. Stillhart, B. Ruiz, R. U. A. Khan, and P. Günter, "Generation of terahertz pulses through optical rectification in organic DAST crystals: theory and experiment," J. Opt. Soc. Am. B **23**(9), 1822–1835 (2006).
25. C. P. Hauri, C. Ruchert, C. Vicario, and F. Ardana, "Strong-field single-cycle THz pulses generated in an organic crystal," Appl. Phys. Lett. **99**(16), 161116 (2011).
26. O. P. Kwon, S.-J. Kwon, M. Jazbinsek, F. D. J. Brunner, J.-I. Seo, C. Hunziker, A. Schneider, H. Yun, Y.-S. Lee, and P. Günter, "Organic phenolic configurationally locked polyene single crystals for electro-optic and terahertz wave applications," Adv. Funct. Mater. **18**(20), 3242–3250 (2008).
27. P.-J. Kim, J.-H. Jeong, M. Jazbinsek, S.-B. Choi, I.-H. Baek, J.-T. Kim, F. Rotermund, H. Yun, Y. S. Lee, P. Günter, and O. P. Kwon, "Highly efficient organic THz generator pumped at near-infrared: Quinolinium single crystals," Adv. Funct. Mater. **22**(1), 200–209 (2012).
28. C. Vicario, B. Monoszlai, M. Jazbinsek, S. H. Lee, O. P. Kwon, and C. P. Hauri, "Intense, carrier frequency and bandwidth tunable quasi single-cycle pulses from an organic emitter covering the Terahertz frequency gap," Sci. Rep. **5**(1), 14394 (2015).
29. J.-H. Jeong, B.-J. Kang, J.-S. Kim, M. Jazbinsek, S.-H. Lee, S.-C. Lee, I.-H. Baek, H. Yun, J. Kim, Y. S. Lee, J.-H. Lee, J.-H. Kim, F. Rotermund, and O. P. Kwon, "High-power broadband organic THz generator," Sci. Rep. **3**(1), 3200 (2013).
30. J. Lu, H. Y. Hwang, X. Li, S.-H. Lee, O. P. Kwon, and K. A. Nelson, "Tunable multi-cycle THz generation in organic crystal HMQ-TMS," Opt. Express **23**(17), 22723–22729 (2015).
31. F. D. J. Brunner, S. H. Lee, O. P. Kwon, and T. Feurer, "THz generation by optical rectification of near-infrared laser pulses in the organic nonlinear optical crystal HMQ-TMS," Opt. Mater. Express **4**(8), 1586–1592 (2014).
32. A. Krueger and P. Féru, "Laser & sources," Getting Practical – SPIE (2004).
33. G. Chang, C. J. Divin, C. H. Liu, S. L. Williamson, A. Galvanauskas, and T. B. Norris, "Power scalable compact THz system based on an ultrafast Yb-doped fiber amplifier," Opt. Express **14**(17), 7909–7913 (2006).
34. M. C. Hoffmann, K.-L. Yeh, J. Hebling, and K. A. Nelson, "Efficient terahertz generation by optical rectification at 1035 nm," Opt. Express **15**(18), 11706–11713 (2007).
35. J. A. Fülöp, Z. Ollmann, C. Lombosi, C. Skrobol, S. Klingebiel, L. Pálfalvi, F. Krausz, S. Karsch, and J. Hebling, "Efficient generation of THz pulses with 0.4 mJ energy," Opt. Express **22**(17), 20155–20163 (2014).

Optics EXPRESS

36. W. R. Huang, S.-W. Huang, E. Granados, K. Ravi, K.-H. Hong, L. E. Zapata, and F. X. Kärtner, "Highly efficient terahertz pulse generation by optical rectification in stoichiometric and cryo-cooled congruent lithium niobate," J. Mod. Opt. **62**(18), 1486–1493 (2015).
37. C. Vicario, B. Monoszlai, C. Lombosi, A. Mareczko, A. Courjaud, J. A. Fülöp, and C. P. Hauri, "Pump pulse width and temperature effects in lithium niobate for efficient THz generation," Opt. Lett. **38**(24), 5373–5376 (2013).
38. Q. Wu and X.-C. Zhang, "Free-space electro-optics sampling of terahertz beams," Appl. Phys. Lett. **67**(24), 3523–3525 (1995).
39. A. Leitenstorfer, S. Hunsche, J. Shah, M. C. Nuss, and W. H. Knox, "Detectors and sources for ultrabroadband electro-optic sampling: experiment and theory," Appl. Phys. Lett. **74**(11), 1516–1518 (1999).
40. D. E. Aspnes and A. A. Studna, "Dielectric functions and optical parameters of Si, Ge, GaP, GaAs, GaSb, InP, InAs, and InSb from 1.5 to 6.0 eV," Phys. Rev. B **27**(2), 985–1009 (1983).
41. A. Yariv, *Optical electronics in modern communications*, New York, 5th edition, (Oxford University, 1997).
42. H. Zhang, S. Virally, Q. Bao, L. K. Ping, S. Massar, N. Godbout, and P. Kockaert, "Z-scan measurement of the nonlinear refractive index of graphene," Opt. Lett. **37**(11), 1856–1858 (2012).
43. L. Razzari, F. H. Su, G. Sharma, F. Blanchard, A. Ayesheshim, H.-C. Bandulet, R. Morandotti, J.-C. Kieffer, T. Ozaki, M. Reid, and F. A. Hegmann, "Nonlinear ultrafast modulation of the optical absorption of intense few-cycle terahertz pulses in n-doped semiconductors," Phys. Rev. B **79**(19), 193204 (2009).

1. Introduction

Terahertz (THz, 1 THz $=10^{12}$ Hz, corresponding to a wavelength of 300 μm in vacuum) technology has grown dramatically, especially thanks to the development of novel ultrafast THz sources [1]. The potential of such radiation for scientific research and industrial applications has been demonstrated through a plethora of studies regarding e.g., time-domain spectroscopy, molecular dynamics, imaging, telecommunications, chemical sensing, and quality monitoring in manufacturing [2–7]. In this context, intense THz sources can play a key role in providing sufficient signal-to-noise ratio for advanced 2D THz imaging [8,9] as well as real-time THz near-field microscopy [10], and have also been exploited for the recent implementation of ultrafast THz scanning tunnelling microscopy [11]. Furthermore, high THz electric fields of the order of hundreds of kV/cm are necessary to explore the nonlinear regime of THz radiation-matter interactions, as recently shown in several matter systems, including semiconductors [12], graphene [13], topological insulators [14], superconductors [15] and multiferroics [16].

One of the most commonly used mechanism to generate few-cycle THz pulses is optical rectification (OR) in nonlinear crystals [2]. The phase matching condition at 800 nm (the emission wavelength of Ti:Sapphire lasers, which are the most commonly used sources for THz pulse generation) can be satisfied in zinc telluride (ZnTe) [17]. However, the peak electric field of the THz pulses generated in such inorganic crystal reaches a maximum value of the order of ~10 kV/cm when standard amplified Ti:Sapphire lasers with energy per pulse of about 1 mJ are used, due to an intrinsically low conversion efficiency (reported as 3×10^{-5} in [18].). Although higher conversion efficiencies can be obtained exploiting difference frequency generation [19,20], this approach leads to a narrowband emission that is not appropriate for several of the applications listed above, which require few-cycle pulses. To achieve broadband emission and high peak electric fields, of the order of hundreds of kV/cm up to MV/cm, OR in lithium niobate ($LiNbO_3$) crystals can be employed [21]. However, such highly nonlinear crystal requires a complex non-collinear pumping scheme, which exploits the pump pulse front tilt to ensure phase matching [22]. Recently, high-energy THz pulses have also been obtained by pumping a ZnTe crystal at 1.7 μm, beyond the three-photon absorption edge. Yet, the phase matching condition was again satisfied through the tilt of the pump pulse front imposed by a grating structure directly fabricated on the crystal surface [23].

As a promising alternative for efficient intense THz generation, organic crystals have been proposed [24–27], since they feature a higher nonlinear response than inorganic crystals (e.g., in DAST the nonlinear optical coefficient is d_{11} = 290 pm/V at 1.5 μm, while the electro-optic coefficient is r_{11} = 77 pm/V at 0.8 μm and r_{11} = 47 pm/V at 1.5 μm [24]). These organic

Optics EXPRESS

emitters can be used to generate high THz peak electric fields (up to MV/cm [25]) via OR in a collinear geometry. Nevertheless, the optimal wavelength to fulfill the phase matching condition typically lies in the range 1.3-1.5 μm, usually requiring a further optical parametric amplifier to be coupled to the femtosecond laser system as a pumping source. Recently, the new organic crystal HMQ-TMS (2-(4-hydroxy-3-methoxystyryl)-1-methilquinolinium-2,4,6-trimethylbenzenesulfonate) has been introduced for THz applications [28–31]. Compared to other organic nonlinear optical crystals, HMQ-TMS shows better environmental stability and many advantageous crystal characteristics, providing the possibility of an easy control of the crystal thickness and aperture size [29]. Furthermore, the optimal molecular packing structure of this crystal maximizes its electro-optic response, resulting in a diagonal component of the effective hyperpolarizability tensor ($\beta_{333}^{eff} = 185 \times 10^{-30}$ esu) that is comparable to the state-of-the-art organic crystals (such as OH1, DAST, and HMQ-T [29]). Finally, since HMQ-TMS possesses a large OR phase-matching band, it can also be pumped at wavelengths shorter than those required by, e.g., DAST and OH1 [28], yet keeping a high conversion efficiency.

In this work, we show how ultrafast ytterbium (Yb) laser technology can be effectively used to pump an HMQ-TMS organic crystal to generate few-cycle high-peak-electric-field THz pulses in a simple collinear scheme, an advantageous geometry for many practical implementations. Indeed, fully diode-pumped Yb-based laser systems, emitting at the central wavelength of 1030 nm, are becoming an increasingly important technology in a wide range of industrial and scientific applications, surpassing Ti:Sapphire systems in terms of compactness, lower cost, thermal stability, higher efficiency, and higher output powers [32]. To date, Yb-based lasers are commonly used in combination with GaP crystals for THz generation in a collinear geometry [33]. However, the maximum peak electric field is in this case limited to few kV/cm. While $LiNbO_3$ crystals are also available at 1030 nm for more intense THz generation, they still require a complex pulse front tilt pumping scheme [34–37]. Here, we demonstrate that an HMQ-TMS crystal pumped by an amplified solid-state Yb-doped potassium-gadolinium tungstate (Yb:KGW) laser offers a simple solution for the generation of few-cycle intense THz pulses with peak electric fields of hundreds of kV/cm. In addition, in a proof-of-principle experiment, we show that this source can be straightforwardly employed to investigate THz nonlinear phenomena in condensed matter.

2. Experimental results

In our study, an HMQ-TMS crystal with a thickness of 630 μm was used for the generation of THz pulses. For the THz electric field characterization, we exploited a standard time-domain spectroscopy setup in a nitrogen-purged environment, as shown in Fig. 1. We employed 170-fs-long pulses from an Yb:KGW amplified laser (*Pharos* PH1-SP-1mJ, *Light Conversion*), centered at λ_0 = 1030 nm, with a maximum pulse energy of 1 mJ and a repetition rate set at 500 Hz (controlled by the internal pulse picker, to reduce the average output power and the corresponding thermal load on the crystal). The residual pump radiation after the HMQ-TMS crystal was blocked by means of a 100-μm-thick black polyethylene sheet. The generated THz radiation was collected and finally focused onto a 300-μm-thick <110> GaP crystal by means of a set of gold off-axis parabolic mirrors (OPMs). We acquired the time trace of the THz electric field through the standard electro-optical sampling (EOS) technique [38], exploiting the GaP crystal as the detector, with a delay step of 15 fs. Since the laser output beam waist (4.5 mm in diameter at $1/e^2$ of the intensity) is larger than the clear aperture of the HMQ-TMS crystal (diameter of 3 mm), a pinhole was used to limit the pump beam size to the crystal aperture. We found this configuration more effective than the use of an optical telescope to reduce the pump beam size, since long term exposure of the organic crystal to a pump beam with spot size < 3 mm eventually resulted in local damage and a subsequent reduction of the conversion efficiency.

Optics EXPRESS

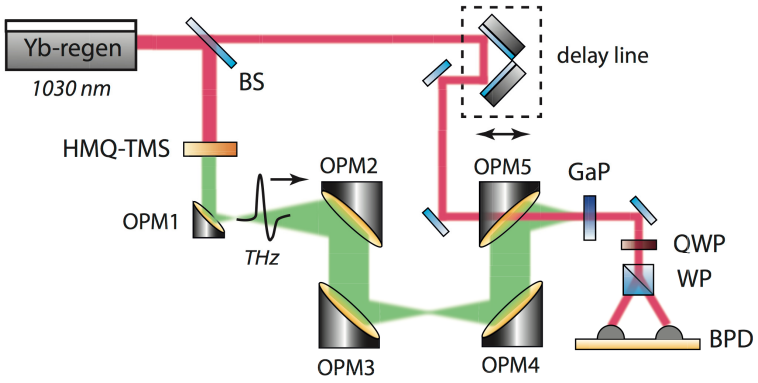

Fig. 1. Schematic of the time-domain spectroscopy setup used for the characterization of the THz pulses emitted by the HMQ-TMS crystal. BS – beam splitter 80:20, OPM – 90-deg off-axis parabolic mirrors (focal length of OPM1: 0.5", OPM2: 6", OPM3 and OPM4: 3", OPM5: 2"), QWP – quarter wave plate, WP – Wollaston prism, BPD – balanced photodiodes. Detection is performed via EOS in a 300-µm-thick <110> GaP crystal.

As it is shown in Fig. 2, this source provides few-cycle THz pulses (Fig. 2(a)) with an emission spectrum extending beyond 3 THz (Fig. 2(b)). The dip located at 1.7 THz in the frequency spectrum is associated with a phonon mode of the HMQ-TMS crystal [28]. In the plane-wave non-depleted pump approximation and ignoring cascaded nonlinear effects, it is also possible to theoretically evaluate the THz spectrum retrieved via EOS in the GaP crystal, following a procedure similar to the one described in [24]. In these calculations, we took into account: the pulse duration of both the pump and probe pulses; the refractive index and absorption coefficient of HMQ-TMS at both optical and THz frequencies [28,31]; the GaP detector response function, considering its THz [39] and optical [40] characteristics. Note that the optimal phase matching wavelength for the electro-optic detection of THz radiation with a GaP crystal nearly coincides with the used probe wavelength (1030 nm). Therefore, a 300-µm-thick detection crystal does not considerably modify the spectrum up to about 5 THz. As it is possible to observe in Fig. 2(b), the experimental and theoretical results show a very good agreement, especially in terms of the overall emission band and the phonon dip position.

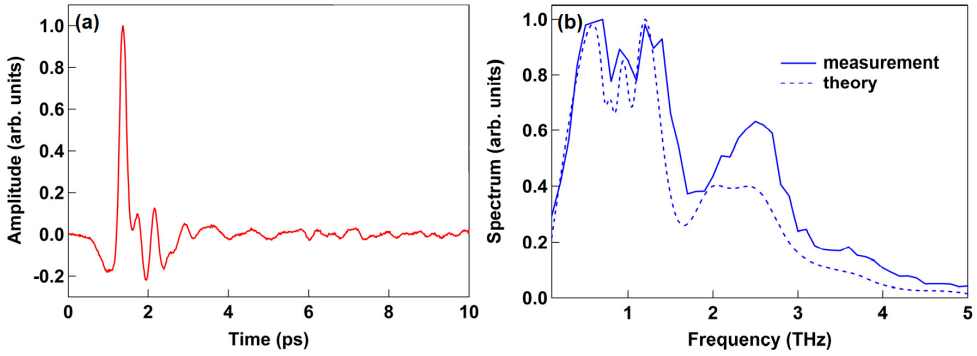

Fig. 2. (a) THz electric field waveform emitted by the 630-µm-thick HMQ-TMS crystal and retrieved via EOS using a GaP detection crystal. (b) Measured (solid) and theoretical (dashed) THz emission amplitude spectra, as retrieved via EOS.

We then quantitatively estimated the strength of the THz peak electric field retrieved through EOS. For small modulations, the differential intensity measured by the balanced photodiodes (see Fig. 1) is directly proportional to the THz field strength, as shown by the following relation [41]:

Optics EXPRESS

$$\frac{\Delta I}{I} = \frac{2\pi d n_0^3 r_{41} t E_{THz}}{\lambda_0} \quad (1)$$

where $\Delta I/I$ is the normalized intensity modulation, E_{THz} is the THz peak electric field, λ_0 is the probe central wavelength, while $n_0 = 3.11$, $t = 0.46$, $d = 300$ µm and $r_{41} = 0.97$ pm/V are the refractive index at λ_0, the THz electric field transmission coefficient, the thickness and the electro-optic coefficient of the <110>-oriented GaP crystal, respectively. In order to avoid over-rotation in the GaP crystal as well as a nonlinear response of the EOS, we attenuated the incident THz signal by placing 2 high-resistivity (> 5000 Ω·cm) silicon wafers in the beam path (each of them providing about 70% of electric field transmission). The measured quasi-linear trend of the THz peak electric field as a function of the pump fluence (defined as the ratio between the incident pump energy on the crystal and the area of the pin-hole) is shown in Fig. 3(a).

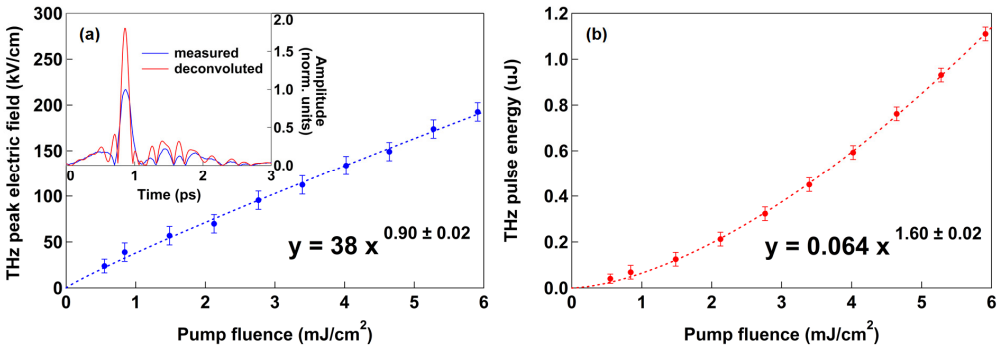

Fig. 3. Peak electric field (a) and energy (b) of the THz pulses generated by the 630-µm-thick HMQ-TMS crystal as a function of the incident pump fluence. The inset of Fig. 3(a) shows the normalized absolute values of the measured THz field (blue) and of a waveform obtained by deconvoluting the measured trace with a Gaussian optical probe of 170 fs - FWHM (red). The formulas reported in both figures represent the best fit of the experimental data (dashed lines).

As it is possible to observe, the maximum THz peak electric field that we measured was around 200 kV/cm. Note that the temporal duration of our optical probe pulse (FWHM of 170 fs) is relatively long and thus does not allow to fully resolve the amplitude of the oscillations of the generated THz electric field. To illustrate this, in the inset of Fig. 3(a) we show the absolute value of the measured electric field trace E_{meas} (blue) compared to the one of a THz waveform E_{dec} (red) obtained by deconvoluting the measured trace with a Gaussian optical probe G of 170 fs (FWHM), according to the formula: $E_{meas} = E_{dec} * G$. As it is evident from this evaluation, the effective THz peak value can be up to 1.8 times higher than the one extracted from our EOS measurement, which corresponds to a maximum peak electric field of about 350 kV/cm at the detection crystal position. We also measured the THz pulse energy by means of a pyroelectric detector (THZ-I-BNC from *Gentec-EO*). The generated THz energy is presented in Fig. 3(b), showing a super-linear dependence on the pump pulse fluence. At the maximum incident pump fluence of about 5.9 mJ/cm^2 (well below the damage threshold previously reported for the HMQ-TMS crystal, i.e. > 20 mJ/cm^2 [28]), the generated THz pulses reach an energy value of about 1.1 µJ per pulse (average power of 550 µW at 500 Hz), corresponding to a significant energy conversion efficiency of 0.26% (quantum efficiency of 56% at the THz central frequency of 1.35 THz). It is worth mentioning that the investigated THz generation process can be straightforwardly scaled up, in terms of both THz energy and peak electric field, through the use of larger aperture crystals and higher pump energies.

Optics EXPRESS

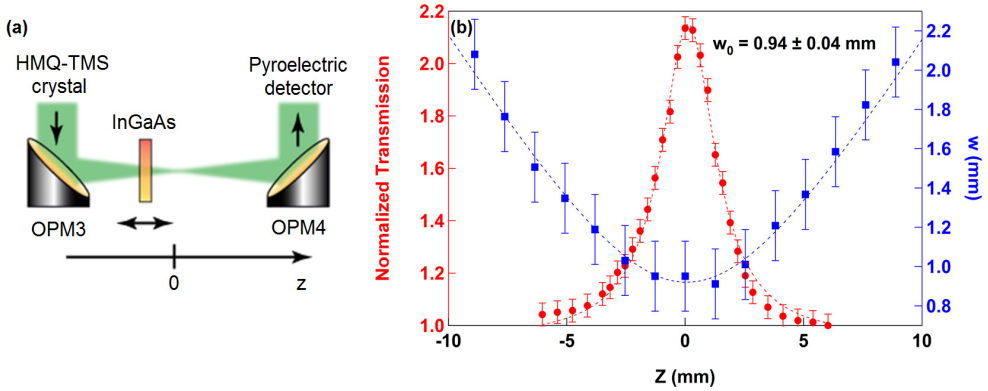

Fig. 4. (a) Schematic of the setup for the Z-scan measurement. (b) Normalized transmission of the InGaAs epilayer (red points) and THz beam size values (blue points) measured as a function of the z position (z = 0 corresponds to the THz focal position).

In order to demonstrate the potential of this source for nonlinear THz investigations, we performed an open-aperture Z-scan experiment on a 500-nm-thick n-doped InGaAs epilayer (carrier density n ~2×10^{18} cm^{-3}) deposited on an InP substrate. Indeed, Z-scan is a very common nonlinear optical characterization technique that enables, for instance, the determination of the Kerr nonlinearity as well as the nonlinear absorption coefficients of a material from intensity-dependent transmission changes [42]. In our measurement, we recorded the THz energy transmitted through the sample while it was scanned along the propagation direction *z* across the focused THz beam (see Fig. 4(a)). For the selected sample, the strong THz field can induce an intervalley transition (from the Γ to the L valley) of the carriers within the InGaAs conduction band. The carrier mobility is lower in the satellite L valley, thus resulting in a lower conductivity of the film (i.e., a higher THz transmission) [43]. For each point of the scan along the *z* direction, we extracted the normalized transmission as the detected transmitted energy divided by the value measured at low THz intensity (i.e., away from the THz focus, at one extremity of the scanned range). The results of this measurement are shown in Fig. 4(b) (red circles). We observed a significant saturation of the THz absorption, with a maximum transmission increase of about 2.2 times at the focus. This transmission change is related with the change of the THz beam size (and the subsequent change in its intensity) along the *z* direction between OPM3 and OPM4. Such size was estimated by performing knife-edge measurements on the THz beam at different *z* positions, by monitoring the transmitted energy with the pyroelectric detector. The results of this characterization are also shown in Fig. 4(b) (blue squares). In this way, we retrieved a THz beam waist of 940 μm (radius at $1/e^2$ of the intensity) at the focal position of OPM3. In a previous Z-scan experiment performed on the same sample [43] (using THz pulses generated via OR in a large-aperture ZnTe crystal pumped by 30 mJ, 30-fs-long optical pulses at 800 nm), a similar increase in THz transmission was found for a peak electric field of around 200 kV/cm. This value is in fair agreement with our EOS measurement. Indeed, considering the longer focal length of OPM3 (f = 3") in comparison to OPM5 (f = 2"), the THz beam waist at the Z-scan sample position is 1.5 larger than the one at the GaP detection crystal (a value also confirmed by an additional knife-edge measurement, not shown). Thus, the THz peak electric field that we can estimate from our EOS characterization at the Z-scan sample position is about 230 kV/cm (taking into account the deconvolution factor mentioned above). A direct quantitative comparison with the experiment reported in [43] is however difficult, due to differences in the temporal and spectral shapes of the THz pulses employed in the two cases, which can also affect the nonlinear response of the doped InGaAs sample. That said, this

Optics EXPRESS

characterization further confirms the significant electric field strength of the emitted THz pulses and shows how they can be effectively employed for nonlinear THz studies.

3. Conclusion

Yb lasers surely represent the new frontier of ultrafast laser technology [32], but their exploitation for the efficient generation of THz radiation is still limited to complex pumping schemes, due to the fact that the most common, highly-nonlinear OR crystals do not offer a good phase-matching at 1030 nm. In this work, we have shown that the recently-developed organic crystal HMQ-TMS can be effectively employed for the collinear generation of high-peak-electric-field THz pulses using an amplified Yb laser as the optical pump. We have obtained THz peak electric fields greater than 200 kV/cm, a spectral emission extending beyond 3 THz, and a THz energy per pulse of 1.1 μJ, which corresponds to a significant energy conversion efficiency of 0.26%. We have also employed this THz source in a proof-of-principle nonlinear Z-scan experiment, inducing a significant THz absorption bleaching in an n-doped InGaAs thin film, thus showing the potential of this novel configuration for the exploration of THz nonlinear effects in condensed matter.

Funding

Natural Sciences and Engineering Research Council of Canada (NSERC) (Strategic and Discovery Grants); Prima Quebec; Fonds de Recherche du Québec - Nature et Technologies (FRQNT) (Postdoctoral Fellowship: Bourse d'Excellence pour Étudiants Étrangers (PBEEE)-V2); National Research Foundation of Korea (NRF), Korea Government (2014R1A5A1009799, 2016R1A2B4011050, 2009-0093826); ITMO Fellowship and Professorship Program, Government of the Russian Federation (074-U 01); 1000 Talents Sichuan Program, China.